Jour. of the KGS, Vol. 23, No. 9. September 2007, pp. 51~63

Shaft Resistance Characteristics of Rock-Socketed Drilled Shafts Based on Pile Load Tests

현장 말뚝재하시험을 통한 암반에 근입된 현장타설말뚝의 주면마찰력 결정

Seol, Hoon-Il[1] 설 훈 일

Jeong, Sang-Seom[2] 정 상 섬

요 지

암반에 근입된 현장타설말뚝의 주면거동특성을 분석하고자, 편마암질의 풍화암/연암지역에서 현장 말뚝재하시험(압축재하 4회, 인발시험 5회)을 수행하였다. 이를 통해 암반 풍화, 굴착면 거칠기, 말뚝 직경, 재하방향 등의 요소들이 암반 근입 현장타설말뚝의 주면 전단거동을 결정짓는 주요요소임을 확인할 수 있었다. 본 연구에서는 국내에서 수행된 암반 근입 현장타설말뚝의 재하시험 사례를 토대로 국내 암반조건을 반영한 극한주면마찰력(f_{max})을 제안하였다.

Abstract

Behavior of rock-socketed drilled shafts subjected to axial load was investigated on the basis of pile load tests. The emphasis was laid on analyzing the shear load transfer characteristics from the shafts to surrounding rock. Field load tests were performed on nine test shafts under various conditions such as weathering of rock mass, borehole roughness, pile diameters, and loading directions. The borehole roughness at each test site was profiled using a laser borehole profiler. In order to evaluate and to propose ultimate shaft resistance (f_{max}) of drilled shafts in rock of Korean peninsular, also, database of pile load tests was developed by reviewing various literature and technical reports.

Keywords : Pile load test, Rock-Socketed drilled shaft, Shaft resistance, Ultimate unit shaft resistance

1. Introduction

In South Korea, a number of huge construction projects such as land reclamation projects for an international airport, high-speed railways, and many harbor constructions are in progress in urban and coastal areas. Drilled shafts are frequently used in those areas as a viable replacement for driven piles for two applications: deepwater offshore foundations, and foundations in urban areas where the noise and vibration are associated with pile driving. Over 90% of the drilled shafts constructed in South Korea are embedded in weathered or soft rocks. The weathered rocks, which occupy two-thirds of the total land area of the Korean peninsula, are generally the results of the physical weathering of granite-gneiss of varying thicknesses ranging up to 40 m (Kim et al., 1999).

Empirical correlations, proposed by many researchers, between the shaft resistance and the unconfined compressive

1 Graduate Student, Dept. of Civil Engrg., Yonsei Univ., geo_dr@yonsei.ac.kr, Corresponding Author
2 Member, Ph.D., Prof., Dept. of Civil Engrg., Yonsei Univ., soj9081@yonsei.ac.kr

strength (UCS) of rock are most widely used. The form of these empirical relations can be generalized as

$$f_{max} = \alpha \cdot q_u^{\beta} \quad (1)$$

where f_{max} is the shaft resistance, qu is the UCS of the weaker materials (rock or pile), and α and β are empirical factors. The empirical factors proposed by a number of researchers have been summarized by O'Neill et al. (1996) and are shown in Table 1. Most of these empirical relations were developed for specific limited data sets, which may have correlated well with the proposed equations. However, O'Neill et al. (1996) compared the first nine empirical relations listed in Table 1 with an international database of 137 pile load tests in intermediate-strength rock and concluded that none of the methods could be considered a satisfactory predictor for the database.

According to comprehensive studies by Horvath et al. (1983), O'Neill et al. (1996) and Seidel and Collingwood (2001), the shear behavior of rock-socketed drilled shafts is highly influenced by the following parameters: rock strength, borehole roughness, rock mass modulus and Poisson's ratio, discontinuity structure and surface condition of the rock mass, pile diameters, initial normal stress between pile and rock prior to loading, and construction practices. The effects of these factors are emphasized by most investigators and partly considered in numerous empirical relations for evaluating the shaft resistance. However, it is difficult to determine reliably, based on empirical methods, the interaction between above-mentioned factors in calculating the performance of a socketed pile due to the complexity of the interaction. A conservative approach to design is therefore pursued.

Table 1. Empirical factors for shaft resistance (O'Neill et al., 1996)

Design Method	α	β
Horvath and Kenney (1979)	0.21	0.50
Carter and Kulhawy (1988)	0.20	0.50
Williams et al. (1980)	0.44	0.36
Rowe and Armitage (1984)	0.40	0.57
Rosenberg and Journeaux (1976)	0.34	0.51
Reynolds and Kaderabek (1980)	0.30	1.00
Gupton and Logan (1980)	0.20	1.00
Reese and O'Neill (1988)	0.15	1.00
Toh net al. (1989)	0.25	1.00
Meigh and Wolshi (1979)	0.22	0.60
Horvath (1982)	0.20~0.30	0.50

Johnston and Lam (1989) made detailed investigations of the pile-rock interface with the goal of better understanding the shear load transfer based on constant normal stiffness (CNS) shear test. They observed that for a pile-rock interface, shearing results in dilation as one asperity overrides another. If the surrounding rock mass is unable to deform sufficiently, an inevitable increase in the normal stress, $\Delta\sigma_n$, occurs during shearing. This so-called normal stiffness K_n can be determined conventionally by theoretical analysis of an expanding infinite cylindrical cavity in an elastic half-space (Boresi, 1965) as follows:

$$K_n = \frac{\Delta\sigma_n}{\Delta r} = \frac{E_m}{r(1+\nu_m)} \quad (2)$$

where, $\Delta\sigma_n$ is the increased normal stress, Δr is the dilation, r is the radius of a pile, and E_m and ν_m are the deformation modulus and the Poisson's ratio of the rock mass, respectively. Clearly, greater socket roughness will result in larger dilation for any given pile settlement once sliding at the pile–rock interface has commenced. The CNS boundary condition produces an increase in stress normal to the interface and a corresponding increase in the frictional resistance between pile and rock. For reasonable design of rock-socketed drilled shafts, as a result, it should be considered CNS conditions (Lam, 1983; Ooi and Cater, 1987; Seidel et al., 1995).

2. Site Investigation

Field test sites lie within the new city of Dongtan, which was formerly Hwaseong Formation of Cambrian age. The Hwaseong Formation, which represents bedrock material, is composed primarily of gneiss. The bedrock is exposed without overburden soil because site development was conducted at the test sites. These two test sites (C and M) are about 300 m apart.

To identify the subsurface materials, the subsurface investigation was performed on two boreholes at each test

site. At site C, the rock mass was very closely fractured, with an average rock quality designation (RQD) of about 0%, and was classified into completely weathered rocks on the basis of weathering grades (ISRM, 1981). At site M, the rock mass consisted of moderately weathered gneiss and was typically very closely fractured, with an average RQD of 14%.

In order to evaluate rock mass properties quantifiably in which test piles would be placed, uniaxial compressive tests (UCT), point load tests (PLT), pressuremeter tests (PMT) were carried out, and rock quality designation (RQD), rock mass rating (RMR), rock mass quality (*Q-value*), and *geological strength index (GSI)* were estimated. Test results based on site investigations are summarized in Table 2.

3. Test Pile Installation

A total of nine drilled test shafts were installed in the exposed bedrock of two test sites; five shafts were constructed in completely weathered rocks and the others were done in moderately weathered rocks. Construction condition of all test shafts is summarized in Table 3.

3.1 Test Pile Subjected to Compressive Load

Four of the test piles in completely weathered rock were installed to perform the compression load tests. A schematic *representation of an instrumented drilled shaft subjected* to a compressive load test is shown in Figure 1. The holes,

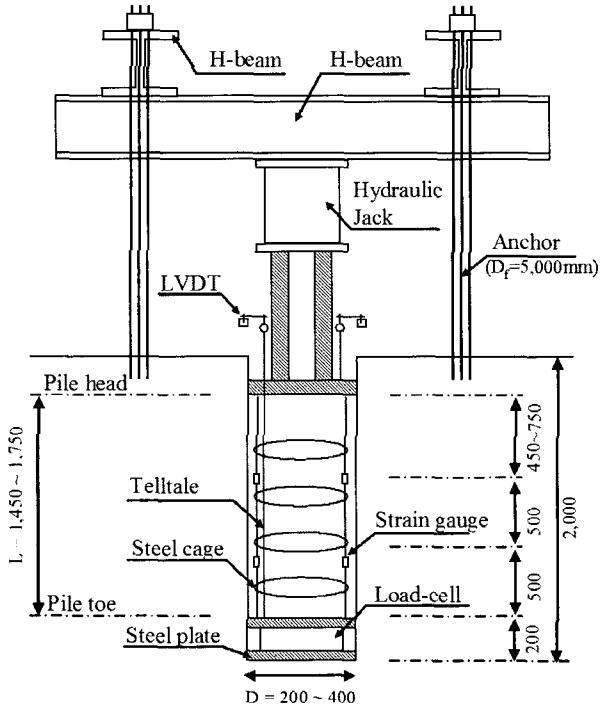

Fig. 1. Test pile detail subjected to axial compressive load

Table 2. Summary of material properties

Test site	Rock type[a]	UCS (MPa)	E_m (MPa)	D_{mass} (MPa)	RQD (%)	RMR	Q	GSI
C	CW	5[b]	271.9	141.2	0	–	–	–
M	MW	50.3	527.2	252.8	14	34	1.08	36

[a] CW: completely weathered; MW: moderately weathered (ISRM, 1981)
[b] Value correlated by PLT

Table 3. Summary of test piles

Test site	Pile No.[a]	Rock Type	Pile Dia. (m)	Pile Leng. (m)	Roughness	Loading method
C	CLSC	CW	0.4	1.75	Smooth	Comp.
	CLRC			1.45	Rough	
	CSSC		0.2	1.75	Smooth	
	CSRC			1.75	Rough	
	CSSU			2.00	Smooth	Uplift
M	MLSU	MW	0.4	1.00	Smooth	Uplift
	MLRU			1.00	Rough	
	MSSU		0.2	1.00	Smooth	
	MSRU			1.00	Rough	

[a] C/M : completely / moderately weathered rock; L/S: 2.0 m / 4.0 m in pile length; S/R: smooth / rough surface; C/U: comp. loading / uplift loading

200-400 mm in diameter and 2,000 mm in depth, were excavated by wash and rotary techniques. The literature survey indicated that borehole roughness is a very important factor in determining shaft resistance of the rock-socketed drilled shafts. Borehole roughness is influenced by the type of rock encountered, the flaws in the rock (joints and seams), and the type of drilling tool used to excavate the rock. To obtain different degrees of borehole roughness, two rock sockets were artificially roughened by grooving.

Test piles were instrumented with load cells, strain gauges, telltales, and LVDTs to measure the load transfer behavior when subjected to cycles of loading and unloading. The load cell installed beneath the pile toe was used to estimate toe load transferred along the pile shaft, thereby allowing the applied load at the pile head to distinguish between the shaft resistance and the toe resistance. Test piles were reinforced with steel bars and steel links at 200 mm vertical spacing. The reinforcing cage sections, fitted with the strain gauges and telltales, were spliced together and then lowered into the pile bore. When the entire reinforcement cage was lowered, a set of readings were taken for all the instruments to check whether they were functioning.

Concrete with an average 28-day curing strength of 40 MPa was placed. A reaction system for loading was constructed using H-beams, a hydraulic jack, and four anchors. The four anchors were placed 1.5 m away from the test pile in plan and socketed 5 m into rock. A hydraulic jack between the test pile and the H-beam, controlled by a single pressure gauge, was used to apply the load.

3.2 Test Pile Subjected to Uplift Load

Five of the test piles were installed for the uplift loading method; one was founded in completely weathered rock (site C), and the others were installed in moderately weathered rock (site M). A schematic representation of an instrumented drilled shaft subjected to the uplift load test is shown in Figure 2. The holes, 200-400 mm in diameter and 4,000 mm in depth, were excavated by wash and rotary techniques in the same way as the test piles subjected to compressive load.

The test pile at site C was instrumented with strain

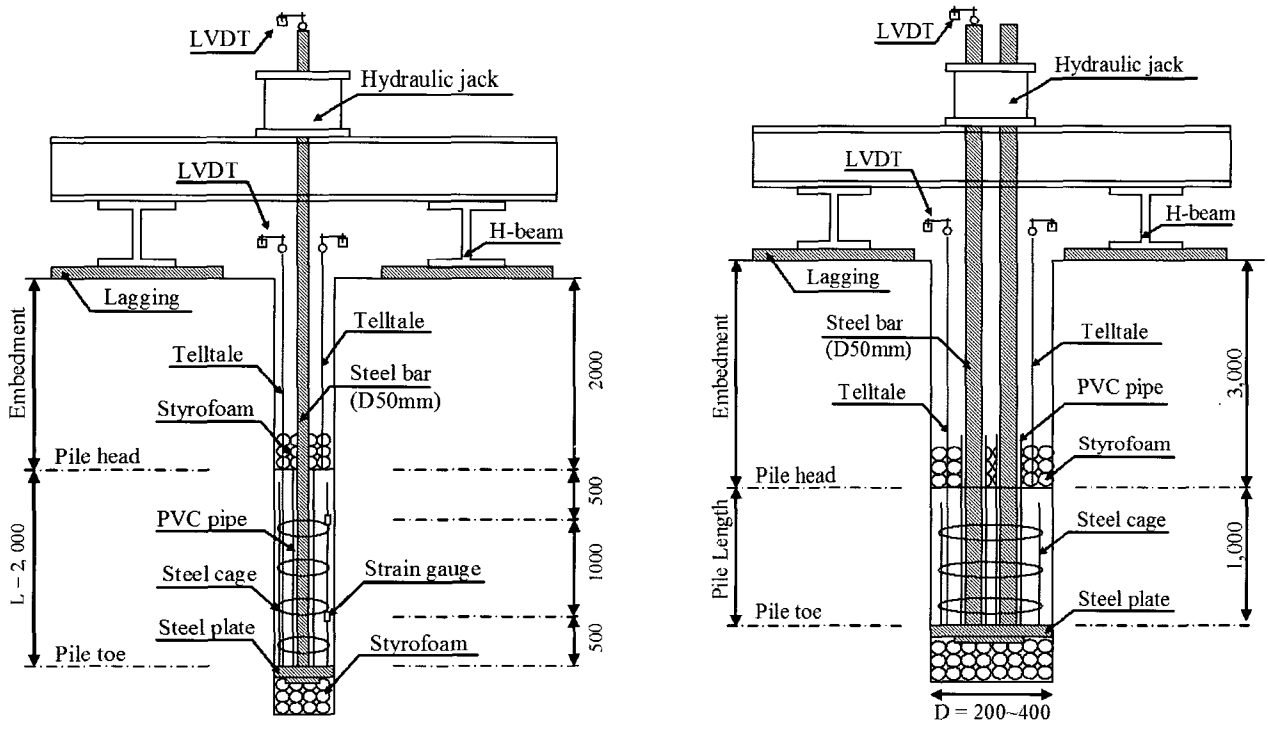

(a) Test pile detail in completely weathered rock

(b) Test pile detail in moderately weathered rock

Fig. 2. Details of test piles subjected to uplift load

gauges, telltales and LVDTs to measure the pile behavior. To apply uplift load directly to the pile toe, the 50-mm-diameter steel bar was instrumented and separated from concrete by polyvinyl chloride pipe. Styrofoam was placed beneath the pile toe and over the pile head, thereby allowing the applied load at the pile toe to transfer along the shaft. The test setup for test piles at site M was the same as test pile at site C except that pile length was 1 m, two steel bars were used to apply loads to test piles 400 mm in diameter without any strain gauge.

Because the material failure of test piles socketed in moderately weathered rock could occur before high ultimate shaft resistance is achieved, high-strength concrete with an average 28-day curing strength of 80 MPa was used.

4. Borehole Roughness Profiling

One of the factors that are known to affect shaft resistance significantly in a rock socket is the roughness of the borehole wall. Some methods for recording surface roughness of the rock mass were noted in the literature review. However, most of these methods are difficult to apply to specific cases, such as in boreholes and for measuring micro-objects for roughness. In this study the borehole roughness at each test site was profiled by molding the roughness surface and then measuring with the laser roughness profiler (LRP). Through comparison with the profiling results of this and other studies, the quantification of borehole roughness in rocks was performed.

4.1 Test Procedure

Alginate and industrial gypsum were used to mold the roughness surface. Alginate has the property of hardening when it is mixed with water. It is convenient to mold the roughness of the borehole wall in the field, because hardening occurs within 2 minutes, and the viscosity is very high. However, the molded alginate sample needs to be imprinted with industrial gypsum plaster, because this type of sample dehydrates causes shrinking and cracking after 2 hours. The long-term strength and deformation of

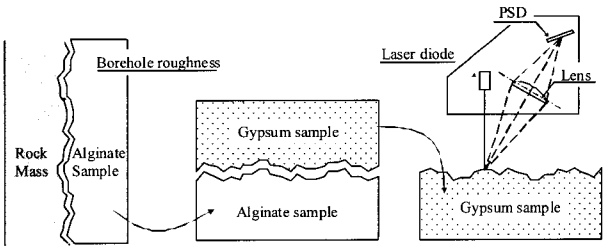

Fig. 3. Schematic of borehole roughness profiling

industrial gypsum are independent of time once the chemical hydration is completed.

Gypsum samples with the molded roughness surface were profiled by using the LRP developed by the Hyundai Institute of Construction. The LRP system was based on the laser triangulation principle. The hardware included a laser generator, a position-sensitive device (PSD) as a laser detector, signal processing circuits, laser control circuits, data acquisition, and digital control units. The accuracy of the roughness measurement was better than 0.1 mm in both the vertical and radial directions. Figure 3 shows the schematic of the borehole roughness profiling.

4.2 Test Results

The roughness profiles for all impressed samples were measured with approximately 0.25 mm intervals in the vertical distance. Sporadic spurious signals, as sharp spikes of very short wave lengths, were filtered out of the data set.

Representative roughness profiles at each site are shown in Figures 4 and 5. It is indicated that rock sockets could be artificially roughened by grooving and the borehole roughness of moderately weathered rock was relatively rougher than those of completely weathered rock. This may have been because there were many vertical discontinuities in moderately weathered rock, so that rock scraps came off the borehole wall.

5. Pile Load Test and Test Results

5.1 Test Procedure

After 32 and 40 days had elapsed since construction

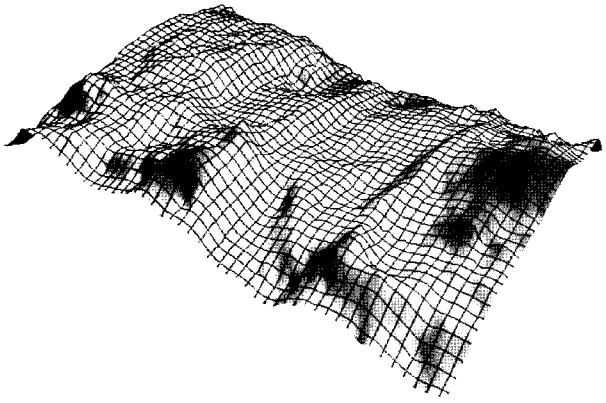

(a) Smooth socket

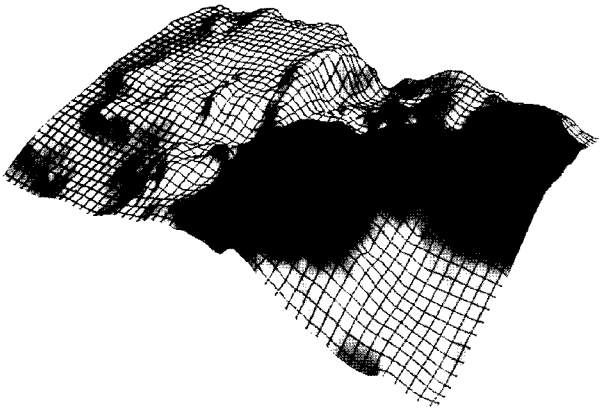

(b) Rough socket

Fig. 4. Typical roughness profiles measured with LRP at site C

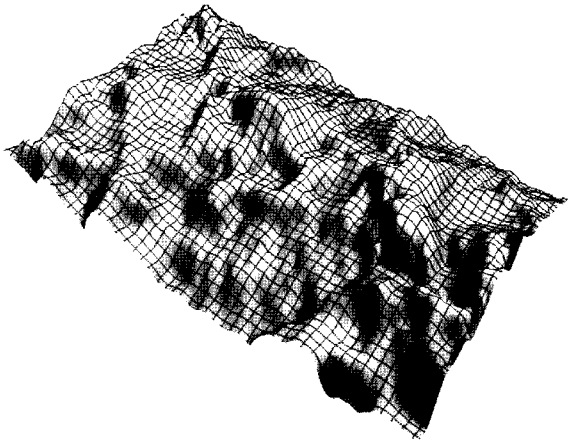

(a) Smooth socket

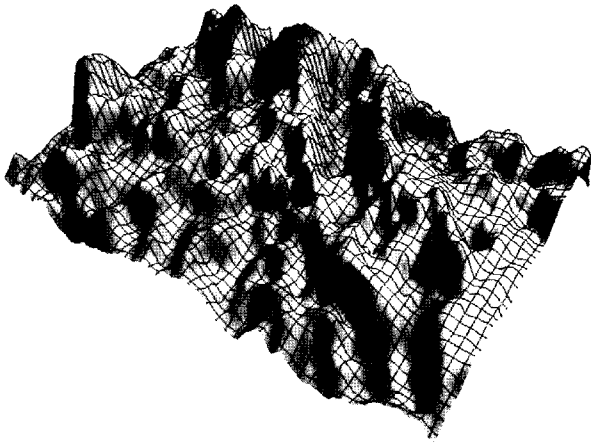

(b) Rough socket

Fig. 5. Typical roughness profiles measured with LRP at site M

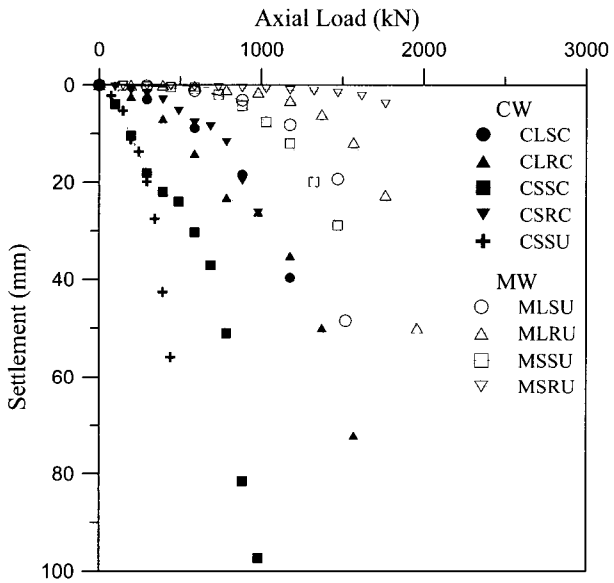

Fig. 6. Pile load test results

of the test piles, load tests were performed at the completely weathered rock site and the moderately weathered rock site, respectively.

Static compressive and uplift load tests performed up to the maximum load of 2,000 kN with four or five unload-reload cycles were designed by the quick-load test method stated in ASTM D1143-81. Figure 6 shows the entire set of the pile load test results omitting the unload-reload cycles.

5.2 Test Results and Discussion

It can be assumed that the shaft resistance of test piles is uniformly distributed along the shaft and that elastic compression is neglected owing to the short length of the test pile. Therefore, the relationship between load transfer and shaft displacement for a short increment along the shaft can be generated by plotting: for each test load, the average load transfer over the increment versus the average displacement of the increment.

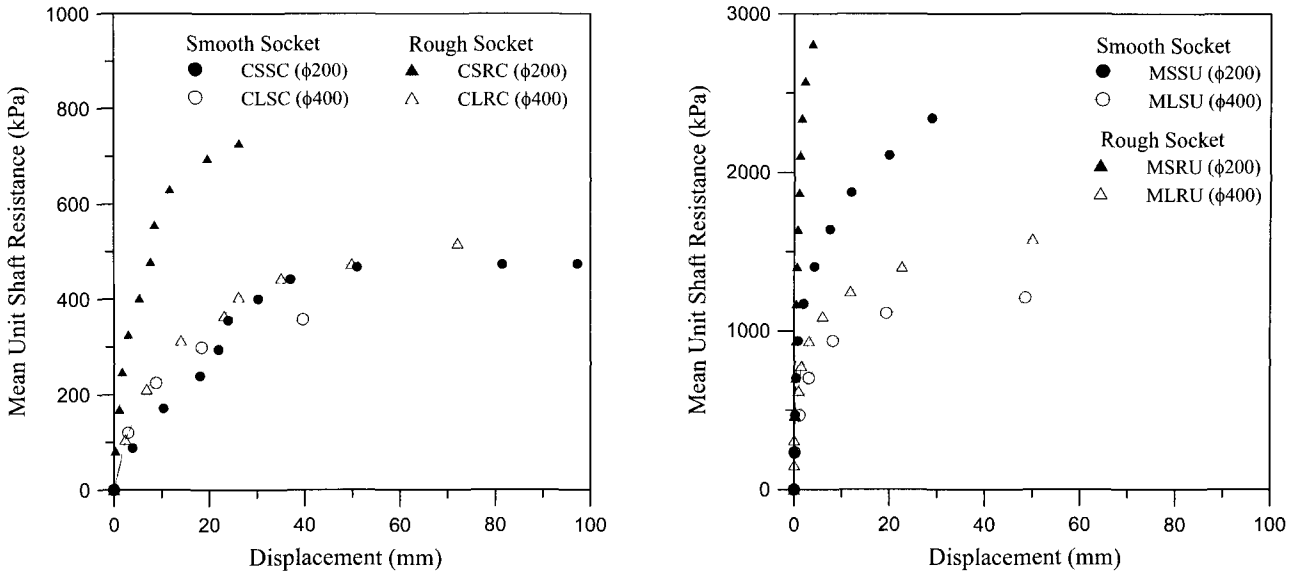

(a) Shafts socketed in completely weathered rock

(b) Shafts socketed in moderately weathered rock

Fig. 7. Mean unit shaft resistance with settlements of pile head

Figure 7 shows the unit shaft resistance-displacement curves for nine test piles embedded in rocks with rough and smooth interfaces. For the moderately weathered rock (see Figure 7b), shaft resistance increased sharply within the displacement of 2 mm, beyond which it continued to increase gradually as displacement increased. On the other hand, the corresponding curve for the completely weathered rocks (see Figure 7a) shows a slow initial increase of shaft resistance for which it is difficult to define inflection points. It is noticed that beyond the initial increase, shaft resistances for the rough sockets increase rapidly toward the failure state and achieve larger f_{max} with respect to f_{max} for the smooth sockets. The reason for this behavioral difference between rough and smooth sockets is explained by the fact that the rough interface produces more dilation, so that shearing resistance occurs more than at the smooth interface. In Figure 7, it is also observed that mean unit shaft resistance of 200-mm-diameter piles tends to increase sharply and achieves a larger value than that of 400-mm-diameter piles, regardless of rock properties and geometry. This might be explained by the fact that normal stiffness of the pile-rock interface increases in proportion to the pile radius (one-half the diameter), as calculated by Eq. 2.

Figure 8 shows a comparison of ultimate unit shaft resistance (f_{max}) of completely and moderately weathered

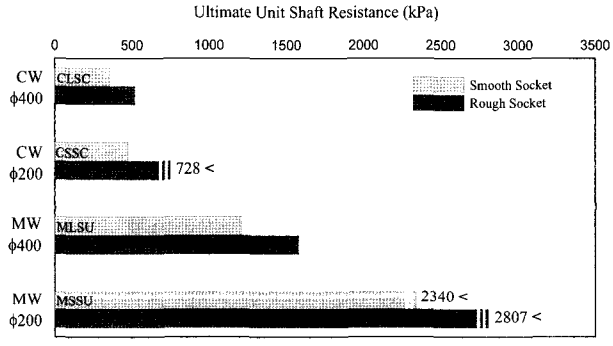

Fig. 8. Effects of roughness and pile diameter

rocks with different roughness and diameters. Among them, test piles of CSRC, CSSU, and MSRU did not reach the ultimate state, so that the maximum test load was applied. It is evident that shaft resistance of test piles, except for CSSC, increases on an average of 36% and 37% as borehole roughness increases or pile diameter decreases, respectively. Also, it is observed that the influence of borehole roughness and pile diameter in moderately weathered rock is larger than in completely weathered rock, owing to stiffness.

Figure 9 shows f-w curves of test piles subjected to compressive and uplift loading. This figure shows that shear behavior by the uplift load test (CSSC) agrees reasonably well with that by the conventional load test (CSSU) for the working load level (within about 20 mm = 10% of pile diameter), beyond which shaft resistance

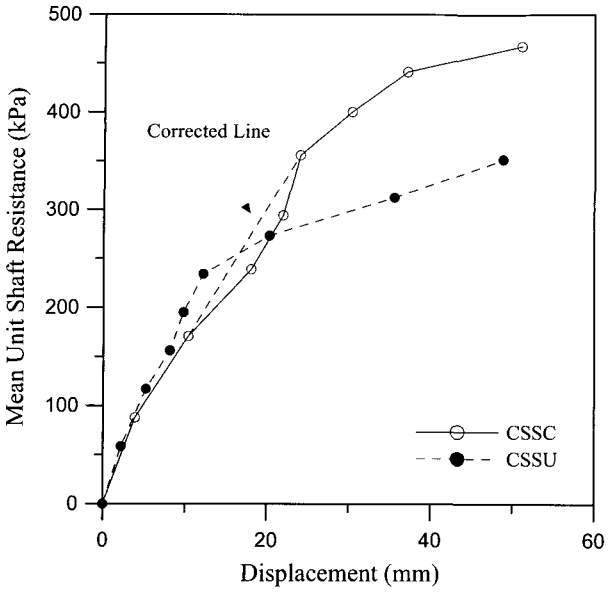

Fig. 9. Effect of loading direction

for the conventional load test increases more than that for the uplift load test. According to the AASHTO design method (1996), ultimate shaft resistance for uplift loading of the rock socket is limited to 70% of the ultimate shaft resistance for compression. Therefore, it is acceptable that shear behavior of the rock socket is not influenced significantly for the working load level by the loading direction, but for the ultimate load level.

6. Database of Pile Load Tests

Numerous empirical correlations between the UCS and the f_{max} of socketed piles measured in load tests have been developed by many researchers as mentioned previously. However, O'Neill et al. (1996) and Nam (2004) concluded that none of the empirical methods could be considered a satisfactory predictor for their database of pile load tests in rock. Their study test sites are mainly sandstone, mudstone, limestone, and clayshale, so that it is required to develop database of load tests on drilled shafts in weathered granite-gneiss, which occupies the whole Korean peninsula, and evaluate characteristics of ultimate capacities.

In this study, therefore, a database on pile load tests was developed by reviewing pertinent literature and reports of load tests performed in rocks of the Korean Peninsula, so that unit ultimate shaft resistance (f_{max}) of rock-socketed drilled shafts was evaluated and proposed. A total of 43 load tests are summarized in Table 4, which gives appropriate information about the load tests, including type of rock, degree of weathering, pile diameter, total pile length, socket length, UCS, E_m, RQD, RMR, f_{max}, and load test method.

6.1 Design Method for Ultimate Shaft Resistance

Representative design methods were identified in this study that will be summarized below (FHWA design method, 1999; NAVFAC DM-7.2 design method, 1982; AASHTO design method, 1996; Canadian Foundation Engineering Manual, 1992). Generally, Korean standards or guidelines for rock-socketed drilled shafts adopt one of these design methods.

(1) FHWA Design Method (1999)

FHWA design method (1999) suggests shaft resistance of rock socket with smooth and rough surface borehole, respectively. For smooth rock socket, the unit ultimate shaft resistance (f_{max}) is determined as (Horvath and Kenny, 1979).

$$f_{max} = 0.65 p_a (q_u / p_a)^{0.5} \leq 0.65 p_a (f'_c / p_a)^{0.5} \quad (3)$$

where, f'_c is the 28-day compressive cylinder strength of the concrete in the socket, p_a is the atmospheric pressure in the units used for q_u, and q_u is median value for UCS along the socket.

For rough (grooved) rock socket, the unit ultimate shaft resistances (f_{max}) are proposed as

$$f_{max} = 0.8 \left[\frac{\Delta r}{r} \left(\frac{L'}{L} \right) \right]^{0.45} q_u \quad : \text{Horvath et al. (1983)} \quad (4a)$$

or

$$f_{max} = \mu p_a (q_u / p_a)^{0.5} \quad : \text{Rowe and Armitage (1984)} \quad (4b)$$

where, L is the socket length, r is the socket radius, Δr is the mean roughness height, L' is the traversed length of the socket, and μ is the adhesion factor (i.e., 0.63: very smooth, 1.42: average, 1.9: artificial grooving).

Table 4. Database of load tests in Korean peninsula

No.	Author	Rock type	Grade[a]	Dia. (m)	Tot. Leng. (m)	Soc. Leng. (m)	UCS (MPa)	E_m (MPa)	RQD (%)	RMR	f_{max} (kPa)	Test method[b]
1	This study	Gneiss	CW	0.2	1.75	1.75	5.0	271.9	0	N/A	474	C
2		Gneiss	CW	0.2	2.0	2.0	5.0	271.9	0	N/A	351	U
3		Gneiss	CW	0.4	1.75	1.75	5.0	271.9	0	N/A	357	C
4		Gneiss	CW	0.2	1.75	1.75	5.0	271.9	0	N/A	728<	C
5		Gneiss	CW	0.4	1.45	1.45	5.0	271.9	0	N/A	518	C
6		Gneiss	HW	0.2	1.0	1.0	50.3	527.2	14	34	2340<	U
7		Gneiss	HW	0.4	1.0	1.0	50.3	527.2	14	34	1209	U
8		Gneiss	HW	0.2	1.0	1.0	50.3	527.2	14	34	2807<	U
9		Gneiss	HW	0.4	1.0	1.0	50.3	527.2	14	34	1580	U
10	Kim et al. (1997)	Granite	CW	0.165	1.0	1.0	N/A	300	0	N/A	147	U
11		Granite	CW	0.165	1.0	1.0	N/A	300	0	N/A	100<	U
12		Granite	CW	0.165	1.0	1.0	N/A	300	0	N/A	130<	U
13		Granite	CW	0.165	1.0	1.0	N/A	300	0	N/A	120<	U
14		Granite	CW	0.165	1.0	1.0	N/A	300	0	N/A	89<	U
15		Granite	CW	0.165	1.0	1.0	N/A	300	0	N/A	106	U
16		Granite	CW	0.165	1.0	1.0	N/A	300	0	N/A	71	U
17		Granite	CW	0.165	1.0	1.0	N/A	300	0	N/A	92	U
18		Granite	CW	0.165	1.0	1.0	N/A	300	0	N/A	77	U
19	Kim (1997)	Gneiss	MW	0.4	9.6	0.5	56	650	40	38	1095	C
20		Gneiss	MW	0.4	10.0	1.1	56	650	40	38	1312	C
21		Gneiss	MW	0.4	10.0	0.8	57	860	40	33	1465	C
22	Cheon (2000)	Gneiss	CW	0.4	10.0	3.0	15.6	62	0	7	428	C
23		Gneiss	CW	0.4	10.2	3.0	15.7	58	0	7	155	C
24		Gneiss	CW	0.4	10.2	3.0	15.7	57	0	7	187	C
25	Kwon et al. (2003)	Brecci	HW	1.5	33.5	5.5	79.0	151	20	28	400<	B
26	Cho et al. (2004)	Gneiss	MW	0.8	2.0	2.0	44	980	40	N/A	1764<	C
27	Kwon (2004)	Gneiss	CW	1.0	13.5	1.3	48.0	905	0	22	670<	C
28		Gneiss	CW	1.0	13.5	1.3	48.0	974	0	22	720	C
29		Gneiss	HW	1.0	13.5	2.1	48.0	1203	9	31	1100<	C
			MW				48.0	1932	40	42	1600	
30		Gneiss	MW	1.0	13.5	1.3	48.0	2748	52	45	1830	C
31	Inchon bridge (2005)	Granite	MW	2.4	45.1	15.2	35	2130	8	N/A	1400<	B
								2300	N/A	N/A	1750<	
32		Granite	MW	2.4	40.0	13.6	30	1480	18	N/A	1400<	B
								1930		N/A	1720<	
33		Granite	MW	3.0	40.1	14.3	54	1630	25	N/A	2370	B
								1300	N/A	N/A	1950	
								1300	N/A	N/A	1630	
34	Song et al. (2005)	Andesite	CW	1.4	16.0	7.0	26.9	N/A	13	N/A	294<	B
			HW			9.0					738<	
35		Andesite	CW	1.4	11.5	6.4	34.4	N/A	9	N/A	250<	B
			MW			5.1					1176<	
36	Ban (2005)	N/A	CW	1.2	29	6.1	N/A	N/A	0	N/A	151<	D
			HW						0		127<	
37		Andesite	HW	0.8	13.9	3.3	N/A	N/A	90	N/A	171<	D
38		Andesite	CW	0.8	17.8	17.8	N/A	N/A	0	N/A	393<	D
			HW						10		56<	
39		Gneiss	CW	1.2	14.8	4.9	N/A	N/A	0	N/A	147<	D
			HW						25		444<	
40		Gneiss	CW	1.5	11.5	4.0	N/A	N/A	0	N/A	195<	D
			HW						0		121<	
41	Seol et al. (2006)	Granite	CW	1.2	26.8	26.8	10	379	5	N/A	433<	B
											820<	
			HW				20	2624	10	N/A	968<	
42		Granite	HW	1.2	9.6	9.6	20	387	10	N/A	671<	B
											928<	
							20	303	10	N/A	320<	
43		Granite	HW	1.2	11.3	11.3	20	865	10	N/A	467<	B

[a] : weathering grade (ISRM, 1981) i.e., CW: completely weathered; HW: highly weathered; MW: moderately weathered; SW: slightly weathered;
[b] : Type of load test i.e., C: conventional load test, U: uplift load test; B: bi-directional load test; D: dynamic load test; < : Not reached ultimate failure

(2) NAVFAC DM-7.2 Design Method (1982)

NAVFAC DM-7.2 design method (1982) describes that unit ultimate shaft resistance (f_{max}) is determined as follows (Horvath and Kenny, 1979)

$$f_{max} = (2.3 \sim 3) q_u^{0.5} \text{ (psi)} \quad \text{for } (D > 406 \text{ mm}) \quad (5a)$$

$$f_{max} = (3 \sim 4) q_u^{0.5} \text{ (psi)} \quad \text{for } (D \leq 406 \text{ mm}) \quad (5b)$$

where, q_u is the UCS of the rock or the concrete shaft, whichever is smaller.

(3) AASHTO Design Method (1996)

The AASHTO design method (1996) prescribes that the ultimate side resistance, Q_{SR}, for shafts socketed into rock is determined using

$$Q_{SR} = \pi B_r D_r (0.144 q_{SR}) \quad (6)$$

where, B_r is diameter of rock socket (ft), D_r is length of rock socket (ft), and q_{SR} is ultimate unit shear resistance along shaft/rock interface (psi), referred to elsewhere herein as f_{max}. q_{SR} is a function of q_u for massive rock. For uplift loading Q_{SR} of a rock socket is limited to $0.7Q_{SR}$ for compression. The design of rock sockets is based on the unconfined compressive strength of the rock mass, q_m, or concrete, σ_c, whichever is weaker. q_m may be estimated using the following,

$$q_m = \alpha_E q_U \quad (7)$$

where α_E is the dimensionless reduction factor for the rock mass (= $0.0231 \cdot RQD - 1.32 \geq 0.15$), and q_u is the UCS of intact rock

(4) Canadian Foundation Engineering Manual (1992)

Canadian Foundation Engineering Manual (CFEM, 1992) proposes unit ultimate shaft resistance as follow.

$$f_{max} = \mu p_a (q_u / p_a)^{0.5} \quad \text{for } (q_u > f'_c) \quad (8a)$$

$$f_{max} = 0.05 f'_c \quad \text{for } (q_u < f'_c) \quad (8b)$$

where, μ is the adhesion factor which is suggested as 1.42 for the average (Rowe and Armitage, 1984) and 0.63 for conservative design (Carter and Kulhawy, 1988).

6.2 Comparison of Predicted and Measured f_{max}

In order to evaluate the various design method in Korea, the measured f_{max} from the database was compared with predicted f_{max} for a certain type of rock in Korean peninsular. The comparisons for f_{max} were made using the methods of FHWA (1999), NAVFAC DM-7.2 (1982), AASHTO (1996), and CFEM (1992), which were mentioned in previous section. Theses design methods mostly utilized only the unconfined compressive strength. Some of the methods have additional design factors (i.e., borehole roughness, RQD, etc.), but because such design factors were not generally reported in the references, those features of the methods were assumed to be intermediate values. Predicted shaft resistances at failure by four design methods were compared with measured shaft resistances at failure for granite, gneiss, andesite, and breccia in the Korean Peninsula, as shown in Figure 10.

The results show that none of the methods gave consistently exact solutions, indicating a wide scatter of the measured versus the predicted values and that most design methods except that of AASHTO (1996) tend to overestimate f_{max}. This is explained, in view of the load-test results from the database, by the facts that (i) design methods for evaluating f_{max} are mostly developed on the basis of specific and limited data sets and (ii) rock masses in the Korean Peninsula have many discontinuities and higher weathering than those in other regions, although the strength of intact rock is relatively high.

6.3 Proposed Unite Ultimate Shaft Resistance

The correlations between f_{max} and UCS of intact rock, E_m, and RMR were plotted, as shown in Figures 11 through 13, respectively. It was found that correlation between f_{max} and UCS of intact rock varies widely but that f_{max} correlates well with E_m and RMR. As mentioned previously, this is because rocks in the Korean Peninsula have many discontinuities and are highly weathered.

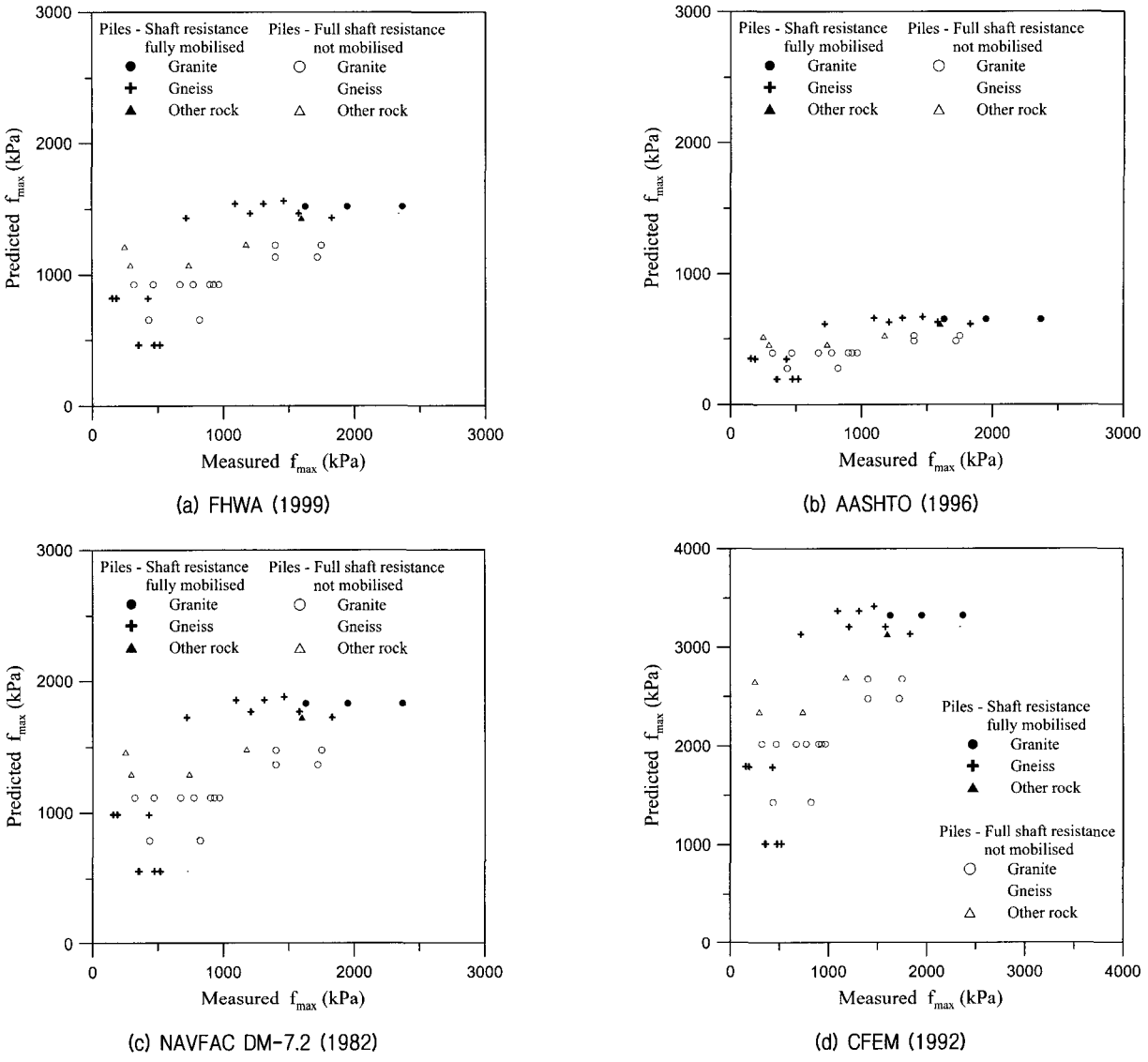

Fig. 10. Comparison of predicted and measured f_{max}

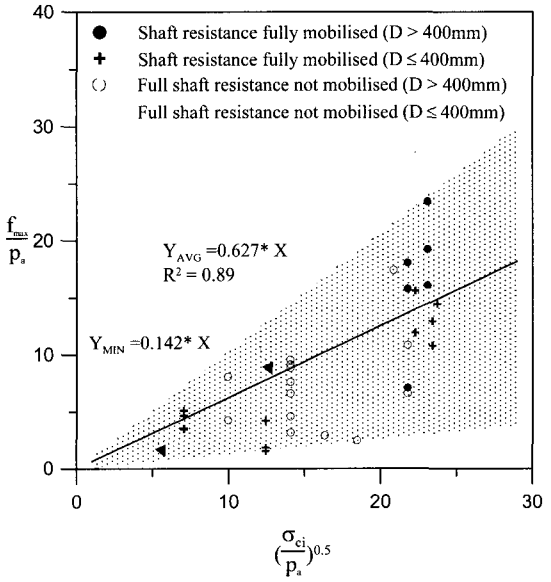

Fig. 11. Variation of f_{max} with UCS of intact rock

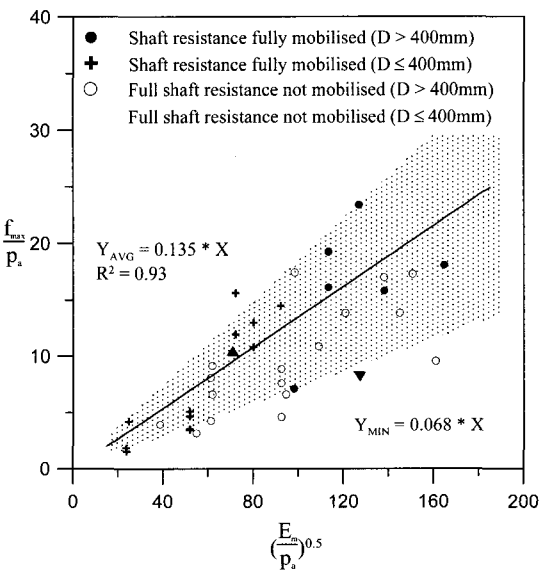

Fig. 12. Variation of f_{max} with E_m

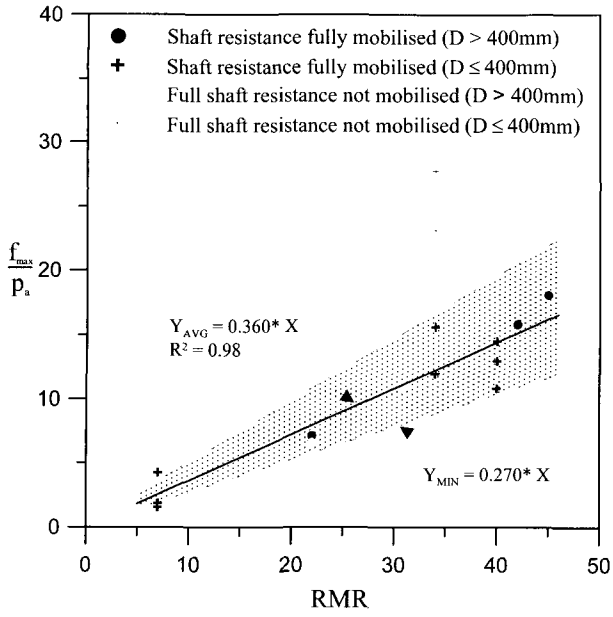

Fig. 13. Variation of f_{max} with RMR

Taking the best linear regressions, as shown in Figures 12 and 13, therefore, the average and minimum f_{max} of rock-socketed drilled shafts in the Korean Peninsula can be proposed as follows:

$$f_{max} = 0.135 p_a \left(\frac{E_m}{p_a}\right)^{0.5} \geq 0.068 p_a \left(\frac{E_m}{p_a}\right)^{0.5} \quad (9a)$$

$$f_{max} = 0.36 p_a \cdot RMR \geq 0.27 p_a \cdot RMR \quad (9b)$$

where, p_a is atmospheric pressure in the units used for E_m

7. Conclusions

In this study, pile load tests were performed on nine drilled shafts under various conditions such as weathering of rock mass, borehole roughness, pile diameter, and loading directions. Also, database was summarized by reviewing various literature and reports of load tests on drilled shafts in rocks of Korean peninsular. Based on the test results and database, the main conclusions are drawn as follows.

(1) Based on the results of pile load tests, it is observed that shaft resistance of rock-socketed drilled shafts increases by an average of 36% and 37% as borehole roughness increases and pile diameter decreases, respectively. However, the influence of borehole roughness and pile diameter decreases, and the initial slope of the f-w relation slows as the degree of weathering increases.

(2) Through comparing results of load tests on piles subjected to compressive and uplift loading, it is acceptable that the shear behavior of the rock socket is not influenced significantly for the working load level (within 0.1D of displacement) by the loading direction but for the ultimate load level. At failure, the shaft resistance for the rock socket by uplift loading was found to be 70% of those by compressive loading, corresponding to limited f_{max} in the AASHTO design method (1996).

(3) Through a developed database of field load tests on drilled shafts in rock of the Korean Peninsula, it is shown that commonly used design methods for calculating f_{max} by using only UCS can substantially overestimate the f_{max} in realistic situations. This could be due to the fact that rock masses in the Korean Peninsula have many discontinuities and greater weathering than in many other regions, even though the strength of intact rock is relatively high. On the other hand, the empirical correlations with rock-mass modulus and RMR in this study are appropriate and realistic to represent the ultimate shaft resistance (f_{max}) of drilled shafts in rocks in the Korean Peninsula.

References

1. AASHTO (1996), "Standard Specifications for Highway Bridges", Sixteenth Edition, *American Association of State Highway and Transportation Officials*, Washington, D. C.
2. Boresi, A. P. (1965), "Elasticity in engineering mechanics", *Prentice-Hall*, Englewood Cliffs, N.J.
3. Canadian Geotechnical Society (1992), "Canadian Foundation Engineering Manual", 3rd Edition, *BiTech Publishers*, Vancouver, BC.
4. Carter, J.P. and Kulhawy, F.H. (1988), Analysis and design of drilled shaft foundations socketed into rock, Final report, EL 5918/ Project 1493-4 / Electric Power Research Institute, Conell Univ., Ithaca, NY.
5. FHWA (1999), "Drilled Shafts: Construction Procedures and Design Methods", FHWA Publication No. FHWA-IF-99-025. *Department of Transportation, Federal Highway Administration*, Office of Implementation, McLean, VA.

6. Horvath, R. G., Kenny. T. C., and Kozicki, p. (1983), "Method of improving the performance of drilled piers in weak rock", *Canadian Geotechnical Journal*, Vol.20, pp.758-772.
7. International Society for Rock Mechanics (1981), "Suggested Methods for the Quantitative Description of Discontinuities in Rock Masses", *Pergamon Press*, UK.
8. Johnston, I. W. and Lam, T. S. K. (1989), "Shear behaviour of regular triangular concrete/rock joints-analysis", *ASCE Journal of Geotechnical Engineering*, Vol.115(5), pp.711-727.
9. Kim, S. I., Jeong, S. S., Cho, S. H., and Park, I. J. (1999), "Shear Load Transter Characeteristics of Drilled Shafts in Weathered Rocks", *Journal of Geotechnical and Geoenvironmental Engineering*, ASCE, Vol.125(11), pp.999-1010.
10. Lam T. S. K. (1983), "Shear behaviour of grouted piles in offshore foundations", Ph.D. Thesis, University of Sydney.
11. Nam, M. S. (2004), "Improved design for drilled shafts in rock", University of Houston, Dissertation.
12. NAVFAC (1982), "Foundation and Earth Structures (Design Manual 7.2)", *Department of The Naval Facilities Engineering Command.*
13. O'Neill, M.W., Townsend, F.C., Hanssan, K.M., Buller, A., and Chan, P.S. (1996), Load transfer for drilled shafts in intermediate geomatrials, FHWA-RD-95-172 Draft report U.S. Department of Transportation.
14. Ooi, L. H. (1989), "The interface behaviour of socketed piles", Ph. D. Thesis, University of Sydney.
15. Seidel, J.P., and Haberfield, C.M. (1995), "The axial capacity of pile sockets in rocks and hard soils. Ground Engineering", Vol.28(2), pp.33-38.
16. Rowe, R.K., and Armitage, H.H. (1984), The design of piles socketed into weak rock. Report GEOT-11-84, University of Western Ontario, London, Ont.
17. Seidel, J. P. and Collingwood, B. (2001), "A new socket roughness factor for prediction of rock socket shaft resistance", *Canadian Geotechnical Journal*, Vol.38(1), pp.138-153.
18. Seol, H. I., Jeong, S. S., Lee, G. H., Kim, Z. C., and Lee, Y. G. (2006), "Load-settlement characteristics of offshore drilled shafts using static bi-directional loading test", *Proc. of Int. Offshore and Polar Engineering Conf., ISOPE*, San Francisco, pp.508-514.

(received on Aug. 20, 2007, accepted on Sep. 30, 2007)